The United Nations University

GEOTHERMAL TRAINING PROGRAMME
Orkustofnun, Grensásvegur 9,
IS-108 Reykjavík, Iceland

Reports 1999
Number 13

THE GEOCHEMISTRY OF THERMAL FLUID IN THE GEOTHERMAL FIELD NEAR ALIA AIRPORT IN JORDAN AND SELFOSS GEOTHERMAL FIELD, S-ICELAND

Abdelkarim S. A.S. Saudi
Natural Resources Authority,
P.O. Box 7 & 2220, Amman,
JORDAN

ABSTRACT

Chemical analysis from 26 wells from the area near Alia airport in Jordan were reviewed and the chemical characteristics of the thermal fluid studied. An Icelandic low-temperature geothermal field at Selfoss, was chosen for comparison. All the data were interpreted by the use of the WATCH program for speciation and the construction of mineral equilibrium diagrams and other graphical presentation and classification. The maximum reservoir temperature for the Jordanian wells predicted by calculation of various geothermometers exceeds 100˚C, whereas for the Selfoss geothermal field, its range is from 130 to 150˚C. There is evidence of mixing with cold water in both fields. The thermal fluid in Jordan is of bicarbonate type water with the reservoir rocks being mainly marly and cherty limestone. In the Selfoss geothermal area, which has been used for district heating for fifty years, there has been observed inflow of cold water into the thermal waters during the past years. This is clearly demonstrated by the geochemical study of the waters.

1. INTRODUCTION

The thermal waters near Alia airport (in Jordan) are located in the central part of Jordan and about 30 km to the south of Amman (Figure 1). The area belongs to the wadi Mujib hydrological basin. Numerous boreholes for agricultural purposes have been drilled in the area, most of them with thermal water of temperatures ranging from 30 to 42˚C. The thermal boreholes are located along the eastern end of the Zarqa ma´in area fault zone and close to the other major faults in the area. All boreholes discharge thermal water from the B2/A7 aquifer which consists of intercalated limestone, chert and marl. The upper part of B2 consists of phosphatic limestone. Some of these boreholes have a H_2S smell, others contain iron oxides. Boreholes G1-G26 have been studied and sampled for chemical analysis and their temperature monitored.

The Selfoss geothermal area is a low-temperature area located in S-Iceland. The thermal water has been used for district heating since 1949 for the town, Selfoss. There has been inflow of shallow cold groundwater mixing with the geothermal water after exploitation started. The Selfoss area has experienced gradual cooling due to the intrusion of cold groundwater. By recasing and cementing the drillholes, the damage from cold water inflow through old wells has been eliminated, (Tómasson and

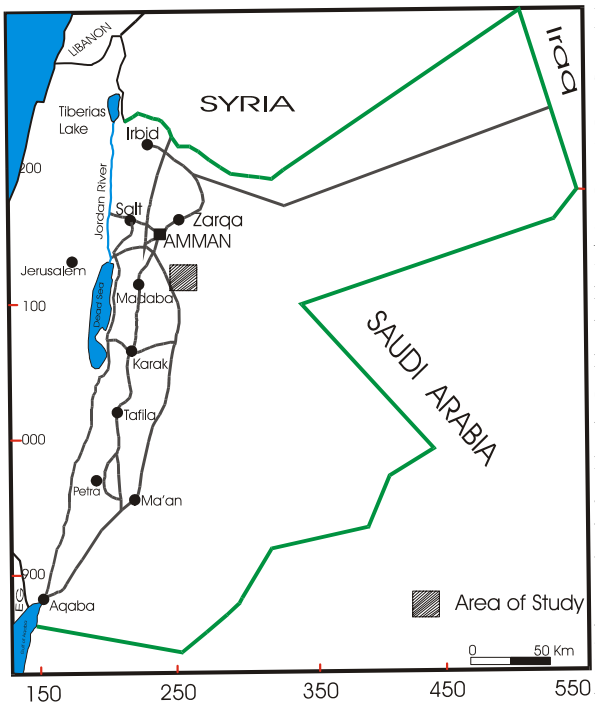

FIGURE 1: Location map of the Alia area in Jordan

Halldórsson, 1981).

The first geothermal investigation in Jordan was carried out by Sir MacDonald. This investigation was limited to wadi Zerqa ma´in and was based on limited chemical analysis. McNitt reviewed the chemical analysis of hot spring water in Jordan collected by the Natural Resources Authority (NRA) in Jordan and recommended a geothermal exploration program in the Zerqa ma´in hot springs field. His recommendation was based on the results of the chemical analysis of a few water samples from the thermal water. In 1977 G. Marionelli, professor of mineralogy of the University of Pisa (Italy), visited Jordan with a team from France and Italy for three weeks, during which they carried out geological and volcanological investigations of the various spring areas and the outcrops for volcanic rocks. During the years 1976-1977, NRA carried out a reconnaissance investigation program, which covered all the main thermal springs and subsurface hot water in Jordan (Swarieh, 1992).

The aim of this study is:

- To study the chemical characteristics of the thermal fluids;
- To assess maximum temperatures;
- To assess potential risk of corrosion or scaling;
- To compare the results with those of the low-temperature geothermal field in Selfoss, S-Iceland.
- To study the potential and technical possibilities and economic interest of heating greenhouses with geothermal heat in Jordan;

2. THERMAL ACTIVITY NEAR ALIA AIRPORT

2.1 Topography

The study area is located about 30 km south of Jordan's capital Amman (Figure 1). The area lies to the east of the main desert highway to Aqaba. The western part of the area and the airport region are easily reached from the main highway which lies west of the map area. The centre and east of the region are crossed by numerous tracks, which allow reasonable access to rugged vehicles in fine weather. The area varies in altitude from a minimum of about 680 m a.s.l. in the westernmost part of the region, to a maximum height of 918 m on Musattarat All Falij in the upper center. The relief is moderate over the area with numerous local rounded peaks between about 800 and 900 m, separated by alluvial flats and wide wades with low angle valley sides. The alleviated valley stretches from the northwest to southeast.

There is a shortage of water; wades flow only in winter, and the stream courses are directed ultimately westwards. Rainfall is demonstrably low, and occurs almost exclusively in winter, sometimes as snow, around 200 mm/year. Regional temperatures are as follows:

Average annual: 17˚C Maximum: 44˚C (June) Minimum: -3˚C (February)

Evaporation is high, relative humidity generally low and the wind raises dust, especially in winter.

2.2 Geological setting

The exposed rocks in the area are wholly sedimentary in origin and upper Cretaceous, lower Tertiary and Pleistocene to Recent in age (Jaser, 1986).

The rock sequence is a succession of shallow marine deposits originally lying in the southern shallow waters of the Tethyan Ocean, and largely consisting of carbonates, which have been moderately tectonically deformed after regression of the sea at the close of the Paleocene, and later eroded by fluvial processes following by uplift (Bender, 1974).

The chronological sequence of lithological units is shown below. The geological data on this report are taken from the 1.50.000, geological map of Khan Ez Zabib, published in 1986.

Alluvial and wadi gravel:	Holocene - Recent
Um Rijam chert limestone:	Eocene
Muwaqqar chalk marl formation:	Paleocene- Tertiary
Al Hisa posphorite formation:	Mastrichtain, upper Cretaceous
Amman silicified limestone:	Campanian, upper Cretaceous

The **Amman silicified limestone** formation occurs as several small outcrops in the mountainous central area. The uppermost part (15-23 m) exposed in the area consists of thin to thick bedded chert, with grey limestone of micritic and wackestone texture, with a thin bed of yellowish marl at the top. The formation was probably deposited in a transgressive sea. Chalks and marls were deposited in deeper water, with the deposition of chert-limestone occurring towards the shore (Futyan, 1968).

The **AL Hisa Phosphorite Formation** consists of more or less silicified phosphorite; phosphorite – bearing oyster lumachelles, and phosphate layers. Chert is less when compared with the Amman formation, where there is a distinct increase in the proportion of limestone and phosphate. Phosphate is locally economically important in Jordan. However, the phosphate bed in this area does not exceed 50 cm and occurs in the upper part of the formations. Soft pelloids and granules in both the phosphatic chert and underlying phosphatic limestone within the formation vary in texture from micrite interbedded with phosphate, to chalky marl. The thickness of this formation is in the range 25-50 m.

The **Muwaquar chalk–marl formation** consists of white chalk, chalky marl, chalky limestone, micritic limestone and Chert. The upper part is interbedded with dark gray to brownish Chert and the lower part consists of thick beds of white to light gray cherts, white chalk with light gray layers and large limestone concretions which reach up to 2 m diameter in places. The thickness of the whole formation is around 70 m. The age is in the range of Maestrichtian-Danian-lower Paleocene, determined by micro-palaentological studies.

The **Um Rijam chert limestone formation** consists of pale yellow to light red chalk marl and chalky limestone, with layers of light grey to grey chert in the form of lenses. The thickness of this formation is around 80 m. The age of the chert limestone is considered to be upper Paleocene-lower Eocene (Bender, 1974).

Alluvial and wadi gravel. The detrital materials of this sediment ranges from coarse–grained and gravel of ill-sorted sub-angular to rounded pebbles. The age is from Holocene to Recent sediments.

2.3 Structural geology

The two **dominant fault trends** within the area are NW-SE and E-W (Figure 2). The Zarqa ma´in fault set is an E-W group of faults and linear features occurring in the central western part of the map area. The Wadi Al-Hammam and the Masattarat AL Falij fault sets represent the major NW-SE trend, and have given rise to the uplifted plateau of the Umm Rijam formation in the northeastern part of the study area,

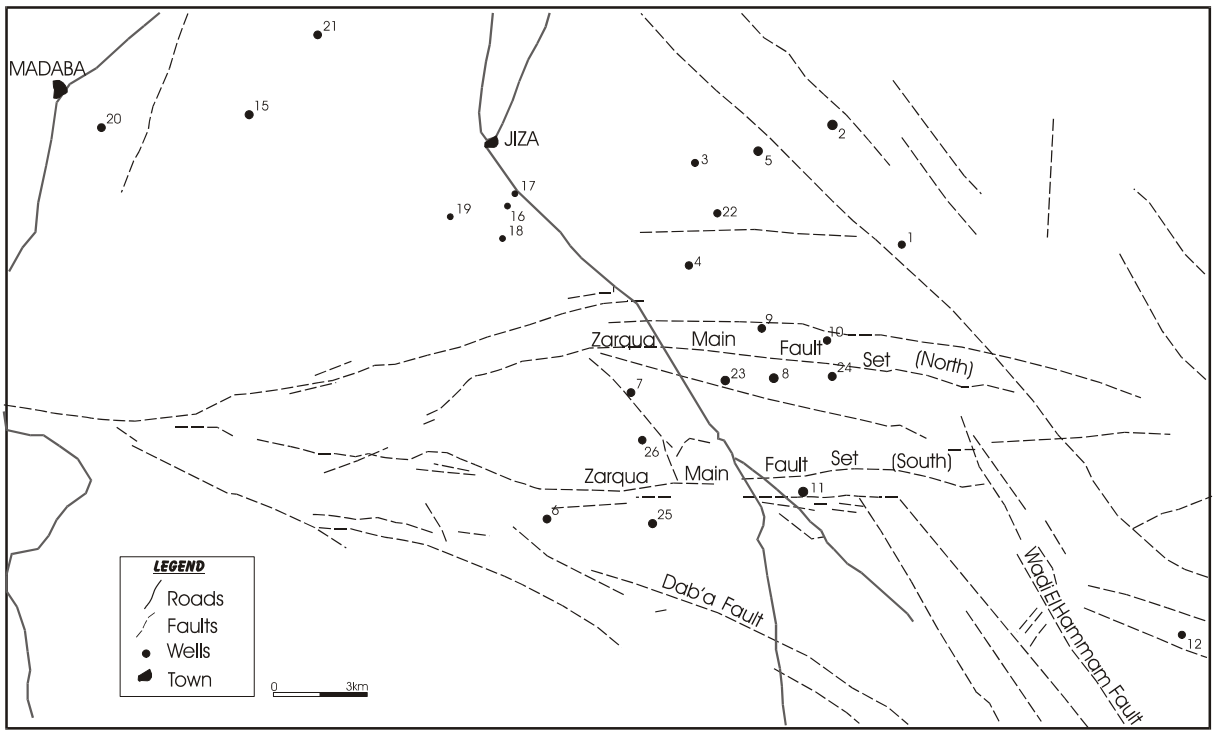

FIGURE 2: Structural sketch map of the studied area (Demange et al., 1992)

and the uplifted area of Muwaqqar chalk marl in the center of the area. Between these two areas of uplift lies the down faulted vale of wadi Al-Hammam.

The folding in the map area is of three types:

1. Gentle folding associated with regional compression.
2. Folding occurring adjacent to faults and directly associated with drag during faulting.
3. Folding in interference structures caused by the interaction of E-W and NW-SE faulting influences.

2.4 Geophysical studies

An **aeromagnetic survey** was done for the whole of Jordan during 1979 by the Phoenix Corporation, and the results were published as maps in scale 1: 100,000 with an interpretation report from the Phoenix Corp. A significant annular positive anomaly was registered in the central south Khan Ez zabib area. This could reflect sulfide or/and oxide mineralisation at depth or a magnetic intrusive body. But there is no evidence for either suggestion. However, an intrusive body could be present within the basement, as Precambrian granite, an ultrabasic body. Or there could be penetration of a part of the overlying strata such as a Tertiary dolerite plug, or a topographic high in the basement surface.

Concomitantly with the magnetic survey, the Phoenix Corporation undertook an **airborne radiometric survey**. There is no obvious correlation between the magnetic and radiometric maps of the area. The radiometric map characteristically reflects surface and nearsurface radioactivity, whereas the aeromagnetic map tends to reflect deeper fundamental features.

Gravity survey data were compiled by Abu Ajamieh (1973) for the central part of Jordan in the scale of 1: 250,000. From the data there can be seen a high positive Bouger gravity anomaly east of the central part of the area which appears to fall south of a major structural break crossing the area from east to west. This structural break could possibly be interpreted as the Zarqa ma´in fault upthrown basement, covered to the south.

3. CHARACTERISTICS OF THERMAL FLUIDS

The composition of thermal fluids depends on many factors. The most important are temperature dependent reactions between host rock and fluid. Leaching also plays an important role when the amount of a particular constituent is too small to achieve equilibrium. At the same time, mixing, boiling and cooling may have a considerably influence on the final composition of thermal fluids.

The boreholes G1-G26 near Alia airport were sampled for chemical analysis for the following elements and compounds; Mg, Ca, K, Na, Cl, SO_4, HCO_3, SiO_2, Li, Mn, F, Br, I, and total dissolved solids (TDS). Field work was carried out by Mr. A. Swarieh (hydrologist) and Mr. R. Massarwah (hydrologist), from the team of geology directorate in Natural Resources Authority of Jordan during the 1990's. Field work has been carried out to monitor the temperature and chemical composition of these boreholes on a monthly basis. This work shows that there is no significant change (> 1˚C) in temperature. The water level contour map of G1-G26 shows that the water flow is to the west and to the centre of the area. There is a drawdown in water level in the middle of the study area due to the high pumping rate. The samples were analysed at the laboratories of the Natural Resources Authority which has a national government qualification in mineral resources, research and analysis of all types of samples.

Results of the chemical analysis from the 26 wells are listed in Table 1, and for comparison Table 2 shows the results of chemical analysis from different locations for cold water. All data from the wells were run by the WATCH program for speciation and calculation of mineral equilibrium. The data were plotted in different triangular classification diagrams, mixing model diagrams etc., and for comparison between chloride content and other components. Eight wells, G1, G6, G8, G13, G14, G18, G21 and G24 were selected for the plotting of mineral saturation log (Q/K) diagrams.

TABLE 1: Chemical composition of geothermal waters near Alia airport in Jordan (concentration in mg/kg)

Well no.	Temp. (˚C)	pH	SiO_2	Na	K	Mg	Ca	Cl	SO_4	HCO_3	F	Br	TDS
G1	41	6.89	30.5	77	3.0	42.5	75	209	95	245	0.1	3.8	845
G2	37	6.75	28.5	70	3.4	40	139	127	92	464	1.4	1.7	960
G3	34	7	44.5	60	2.2	31	67	90	45	310	0.9	2.3	600
G4	35	6.8	20.7	53	2.8	26	100	88	43	451	0.9	0.9	778
G5	37	6.5	44	133	4.1	59	141	248	133	420	1.7	5.4	800
G6	38	6.8	47	157	4.7	53	149	214	208	420	1.6	5.3	1000
G7	33	6.9	44	46	2.9	32	85	75	50	427	1.4	1.0	751
G8	40	6.6	60	112	5.2	55	136	248	202	283	1.4	4.7	1184
G9	33	6.7	43	67	2.3	38.5	109	106	42	434	1.2	3.1	800
G10	37	6.5	49	206	9.6	35	220	418	408	420	1.5	7.6	1900
G11	35	6.7	42.5	240	11.7	80	171	426	382	366	1.6	7.5	1400
G12	40	6.7	41.4	161	7.1	70	174	205	447	439	1.7	3.5	1383
G13	42.5	6.6	81	115	5.3	50	86	178	109	370	1.3	1.6	840
G14	34	6.7	85.6	270	12.1	86	190	408	450	450	1.4	1.8	1700
G15	38	6.9	17	57	7.5	62	39	106	74	285	-	-	750
G16	30	6.9	38	56	2.1	26.5	62	92	20	283	0.5	1.3	600
G17	29	7	43	67	2.4	27	63	92	22	320	0.5	1.2	600
G18	41	6.8	59.5	119	7.0	56.5	142	303	94	374	2.5	9.3	1080
G19	31	7	40	61	2.3	30	63	92	21	320	0.5	1.4	700
G20	38	6.7	40	112	6.2	68	157	184	339	385	3.1	3.7	1356
G21	34	6.7	43.6	87	8.6	35	45	106	25	302	1.1	2.4	600
G22	36	6.1	56	60	6.6	46	67	95	34	370	1.2	1.7	780
G23	37	6.7	12	81	4.4	43	100	-	230	329	1.8	3.6	920
G24	33	6.7	38.4	216	8.1	82	205	369	382	461	1.5	6.9	1661
G25	31	7.2	47	36	2.1	36	78	82	20	342	0.6	1.8	600
G26	36	7.1	44	156	5.1	64	134	214	08	464	1.6	5.3	1253

TABLE 2: Chemical analysis of selected cold springs in Jordan (concentration in mg/kg)

	Na	K	Mg	Ca	Cl	HCO_3	SO_4	F	TDS	pH
Bosaira	52	3.5	28	52	85	215	61	0.5	515	8.5
Dana	17	0.9	20	60	47	254	10	-	430	7.6
Wadi Musa	546	11	115	275	1150	122	600	0.8	2950	7.8
Zerqa ma´in	116	8.1	45	74	177	224	157	0.2	810	-
Wala.3	60	5.1	33	90	92	315	84	-	608	-

3.1 Schoeller diagram

This diagram is used to classify the type of water. It may be also used to show changes over time for the different water types plotted. The log concentrations of fluid constituents from a number of analyses are connected with a line. Because logarithmic values are used, a wide range of concentrations can be shown. The effect of mixing with dilute water (as well as gain or loss of steam) is to move the connecting line vertically without changing its shape (Truesdell, 1991). Different water types will be displayed by crossing lines.

In Figure 3, a Schoeller diagram for water from eight wells, clearly shows bicarbonate waters and suggests mixing between thermal and cold groundwater.

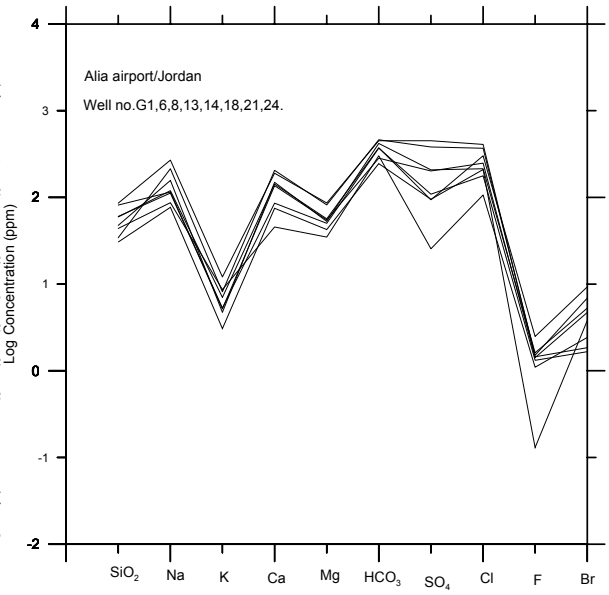

FIGURE 3: Schoeller diagram for thermal waters in Jordan

The Schoeller diagram is prepared according to the percentage of the ions as milliequivalent value. Figure 4 shows Schoeller diagram for the selected cold water samples. It shows a slight range in logarithmic values of potassium, and also represents two types of waters, chloride rich water and sulfate water which represent the Zarqa ma´in area close to the Dead Sea.

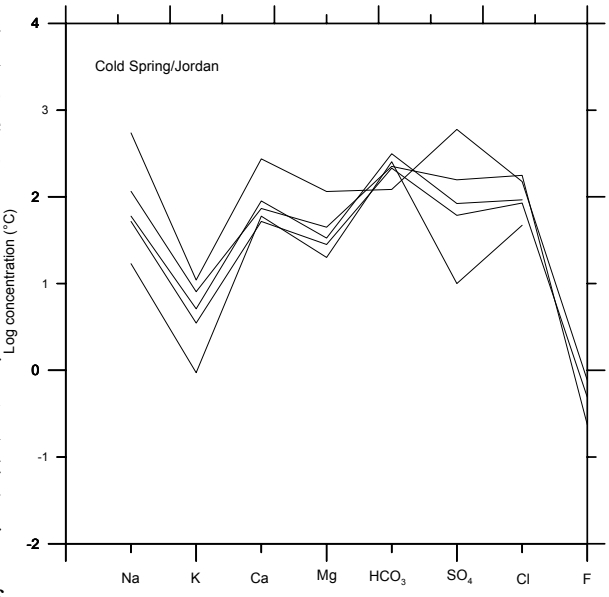

FIGURE 4: Scholler diagram for the selected cold water samples

3.2 Triangular diagrams

The CL-SO_4-HCO_3 diagram. These triangular diagrams are used for the classification of natural waters. This diagram was described by Giggenbach (1991) for the classification of geothermal water. It helps to discern immature unstable waters and may give an initial indication of mixing relationships or geographic groupings. The diagram resembles the popular diagram proposed for the classification of natural waters. It may give a preliminary statistical evaluation of groupings and trends.

The data are plotted by first summing up (S) the concentrations C_i (mg/l) of all three constituents involved, as follows:

$$S = C_{Cl} + C_{SO_4} + C_{HCO_3} \quad (1)$$

The next step consists of evaluations of " *% -Cl* ", " *%-SO4* " and " *%-HCO3*":

$$\%-Cl = 100\,C_{Cl}/S \qquad \%-SO4 = 100\,C_{SO_4}/S \qquad \%-HCO3 = 100\,C_{HCO_3}/S \quad (2)$$

The results of calculations and plotting of analytical research from Alia are shown in Figure 5. Most of the samples plot in the high bicarbonate region or mixed groundwater. The waters of low temperature and four other samples are close to the field of chloride and sulfate waters but are still within the bicarbonate water range which suggests some degree of mixing. Only one sample plots in the chloride field.

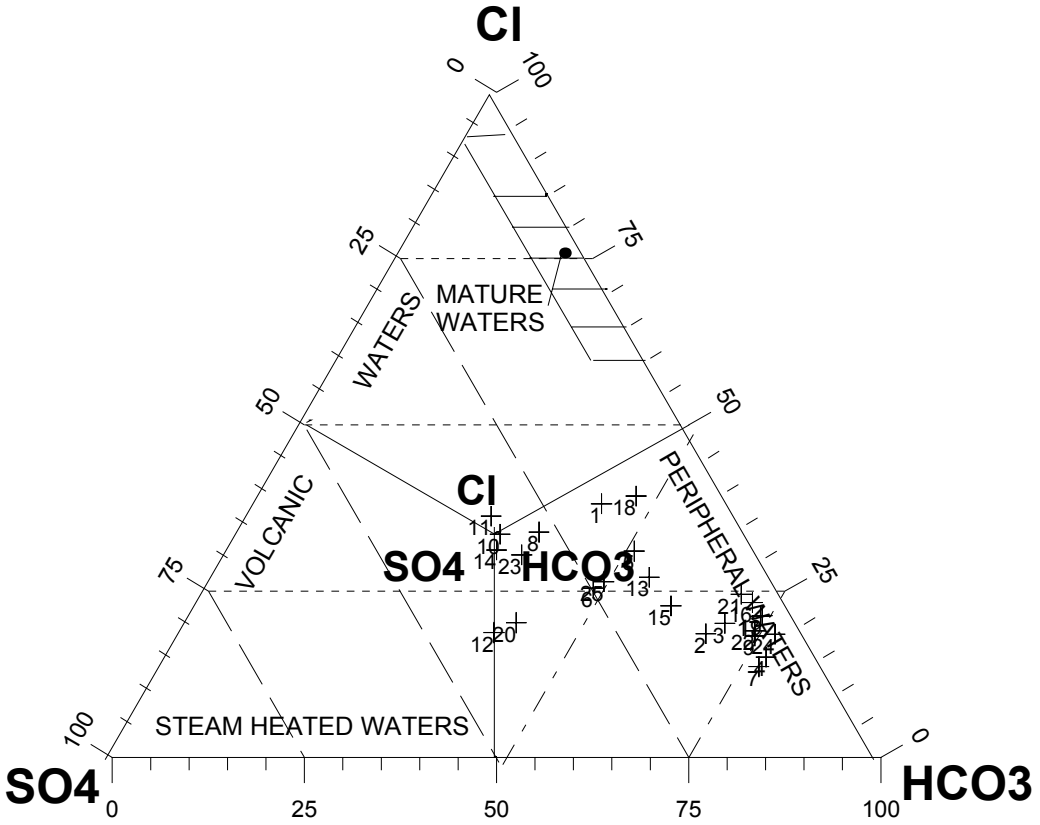

FIGURE 5: The Cl-SO_4-HCO_3 diagram for the thermal waters

The Na-K-Mg diagram was constructed by Giggenbach (1988). It is essentially based on the temperature dependence of the two reactions:

$$K-feldspar + Na^+ = Na-feldspar + K^+ \quad (3)$$

$$2.8\,K-feldspar + 1.6\,water + Mg^{2+} = 0.8\,mica + 0.2\,chlorite + 5.4\,silica + 2K^+ \quad (4)$$

The diagram is used to evaluate equilibrium conditions between the geothermal water and reservoir rocks. The main advantage of this diagram is its ability to picture the position of a large number of samples simultaneously, permitting delineation of mixing trends and groupings. It separates well the position of waters resulting from the two end member processes, rock dissolution and equilibration. As in the other triangular diagram, the sum is calculated to evaluate " *%-Na*" and "*%- Mg*", where C_i i*s* in mg/kg:

$$S = \frac{C_{Na}}{1000} + \frac{C_K}{100} + \sqrt{C_{Mg}} \quad (5)$$

$$\%\text{-}Na = \frac{C_{Na}}{10S} \; ; \quad \%\text{-}K = \frac{C_K}{S} \; ; \quad \%\text{-}Mg = 100\frac{\sqrt{C_{Mg}}}{S} \quad (6)$$

Figure 6 shows that all the samples plot in the area of immature waters, very close to the Mg corner of the diagram, indicating that the thermal fluids are a mixture of cold groundwater. The relatively high Mg concentration is due to the bicarbonate type of the water. Therefore, it is difficult to estimate reservoir temperature.

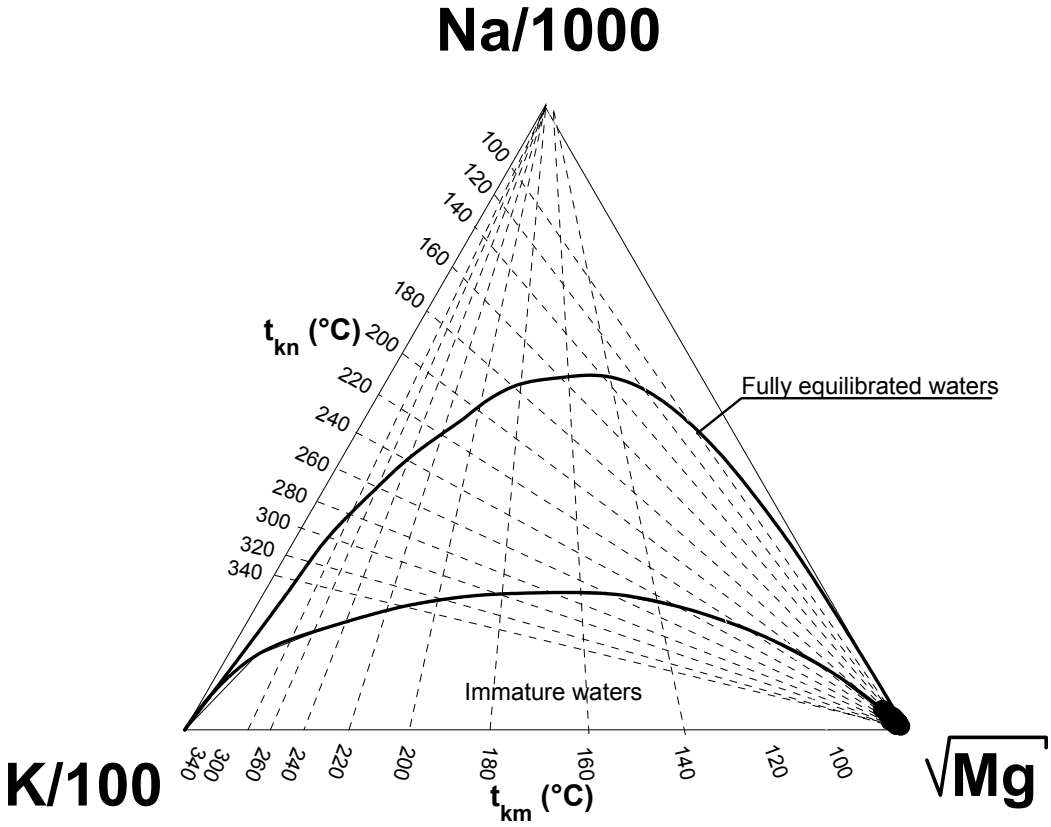

FIGURE 6: The Na-K-Mg diagram for the thermal waters

3.3 Geothermometers

One of the most applied methods in the investigations of geothermal resources involves prediction of subsurface temperature using chemical geothermometers. It is useful to determine the main upflow zones in a geothermal system and the subsurface reservoir temperatures. Cooling of the water may occur by conduction, boiling and/or mixing with cold water, and comparison of different geothermometers may be helpful to interpret those processes. The temperatures in geothermal reservoirs are generally not homogeneous, but variable, both horizontally and vertically, so geothermometry is useful for revealing the temperature of the aquifer feeding the drillholes. Temperatures encountered in a deep drillhole may be higher than those indicated by chemical geothermometry, particularly if the waters investigated are fed by shallow aquifers (Arnórsson, 1991).

3.3.1 Silica geothermometers

The use of dissolved silica as a geothermometer has been derived from experimentally determined variations in the solubility of different silica species in water, as a function of temperature and pressure as well as from observations of well discharges and measured temperature. The basic reaction for the solution of silica minerals to give dissolved silica is:

$$\underset{\textit{Mineral}}{SiO_2(s)} + 2H_2O = \underset{\textit{silicic acid}}{H_4SiO_4(aq)} \quad (7)$$

The silica temperature is based on the equilibrium between quartz or chalcedony and the unionized silica in a thermal fluid. Experiences show that chalcedony temperature is commonly more realistic in low-temperature waters than quartz temperature (Arnórsson, 1975). Both quartz and chalcedony geothermometers were used to estimate subsurface temperatures. The following equations were used:

Quartz - no steam loss (Fournier, 1977)

$$t\,℃ = \frac{1309}{5.19 - \log SiO_2} - 273.15 \quad (8)$$

Quartz - maximum steam loss at 100˚C (Fournier, 1977)

$$t\,℃ = \frac{1522}{5.75 - \log SiO_2} - 273.15 \quad (9)$$

Chalcedony - no steam loss (Fournier, 1977)

$$t\,℃ = \frac{1032}{4.69 - \log SiO_2} - 273.15 \quad (10)$$

Chalcedony - maximum steam loss at 100˚C (Fournier, 1977)

$$t\,℃ = \frac{1182}{5.09 - \log SiO_2} - 273.15 \quad (11)$$

Chalcedony - no steam loss, (Arnórsson et al., 1983)

$$t\,℃ = \frac{1112}{4.91 - \log SiO_2} - 273.15 \quad (12)$$

Chalcedony - maximum steam loss at 100˚C, (Arnórsson et al., 1983)

$$t\,℃ = \frac{1264}{5.31 - \log SiO_2} - 273.15 \quad (13)$$

3.3.2 Cation geothermometers

The **Na-K geothermometer** is based on ion exchange reactions whose equilibrium constants are temperature dependent partitioning of Na and K between hydrothermal altered aluminium silicates and

solutions. The ratio is related to the general exchange reaction

$$K^+ + Na\text{-}feldspar \;=\; K\text{-}feldspar + Na^+ \qquad (14)$$
(albite) (orthoclase)

The equilibrium constant, K_{eq}, for the Equation 14 is:

$$K_{eq} = \frac{[KAlSi_3O_8][Na^+]}{[NaAlSi_3O_8][K^+]} \qquad (15)$$

If the activities of the solid reactants are assumed to be in unity and the activity of the dissolved species is about equal to their molal concentrations, the equation will be reduced to:

$$K_{eq} = \frac{[Na^+]}{[K^+]} \qquad (16)$$

The following formulae, based on empirical correlation, presented by Arnórsson et al. (1983) and Giggenbach (1988), are used in this report; the concentrations of *Na* and *K* are in mg/kg:

Na/K temperature by Arnórsson et al. (1983)

$$t\,℃ = \frac{933}{0.993 + \log(Na/K)} - 273.15 \qquad (17)$$

Na/K temperature by Giggenbach (1988)

$$t\,℃ = \frac{1390}{1.75 + \log(Na/K)} - 273.15 \qquad (18)$$

The **K-Mg geothermometer** is based on the equilibrium between water and the mineral assemblage K-feldspar, K-mica and chlorite (Giggenbach, 1988). It is found that it responds fast to changes in the physical environment and, thus, usually gives a relatively low temperature in mixed and cooled waters as compared to other geothermometers (concentrations are in mg/kg):

$$t\,℃ = \frac{4410}{14.0 - \log(K^2/Mg)} - 273.15 \qquad (19)$$

The **Na-K-Ca geothermometer** was developed by Fournier and Truesdell (1973) for application to waters with elevated Ca contents that give anomalously high calculated temperature for the Na/K geothermometer. The relationships of Na^+, K^+ and Ca^{2+} were explained in terms of Ca^{2+} participating in aluminium silicate reactions, and the amounts of dissolved Na and K are therefore influenced by the dissolved Ca, even though the final amount of aqueous Ca may be controlled largely by carbonate solubility and carbon dioxide (Nicholson, 1988).

The geothermometer is entirely empirical and assumes one type of base exchange reaction at temperatures above about 100˚C (concentrations are in mg/kg):

$$t\,℃ = \frac{1647}{\log(Na/K) + \beta\,[\log(\sqrt{Ca}/Na) + 2.06] + 2.47} - 273.15 \qquad (20)$$

Table 3 shows the results of calculated geothermometers for the waters from the area around Alia airport. The K-Mg geothermometer shows values close to the measured ones. The silica chalcedony geothermometer gives similar values in some cases, but considerably higher in others and lower in one case where the analyse of silica appears to give an odd result. The quartz geothermometer gives considerably higher values than those measured in nearly all cases. It is considered likely that the chalcedony geothermometer gives minimum value for the reservoir temperatures. The Na-K geothermometers may indicate higher temperatures but one cannot rely on the result due to reservoir mixing with cold waters, which makes this geothermometer unreliable.

TABLE 3: Temperature (˚C) of different geothermometers for the thermal waters in the Alia airport wells

Well no.	$T_{meas.}$	T_{quartz} [1]	$T_{chalcedony}$ [2]	T_{Na-K} [3]	T_{Na-K} [4]	T_{K-Mg} [3]
G1	41	77	48	168	126	27
G2	37	80	46	172	132	30
G3	34	96	66	163	120	24
G4	35	64	32	185	147	30
G5	37	96	65	153	108	30
G6	38	99	69	151	106	33
G7	33	96	65	199	166	29
G8	40	111	81	177	137	34
G9	33	95	64	160	116	23
G10	37	101	70	177	138	51
G11	35	94	63	180	142	47
G12	40	93	62	174	135	38
G13	43	125	98	177	137	36
G14	34	128	100	175	135	47
G15	38	56	24	255	242	40
G16	30	91	30	164	122	25
G17	29	95	64	161	118	27
G18	41	110	80	193	158	40
G19	31	91	60	164	122	25
G20	38	92	61	188	152	36
G21	34	95	65	231	208	49
G22	36	107	77	239	219	41
G23	37	45	13	188	1152	34
G24	33	85	53	164	122	39
G25	31	99	68	192	157	22
G26	36	96	65	156	112	33

1) Fournier and Potter, 1982
2) Fournier, 1977
3) Giggenbach, 1988
4) Arnórsson et al., 1983

3.4 Speciation and equilibrium - the WATCH program

The computer program WATCH calculates the speciation of waters at a given temperature. It is quite useful for the interpretation of the chemical composition of geothermal fluids, as well as for non-thermal waters. Some chemical analysis of samples collected at the surface can be used to compute the composition of aquifer fluids. The program calculates aqueous speciation, using mass balance equations and chemical equilibrium. WATCH can also be used to calculate the composition of the sample after cooling or boiling (Arnórsson et al., 1983 and Bjarnason, 1994), and is, thus, useful for modelling the behaviour of water for different design of the geothermal plant.

Three main conditions for geothermal fluids can be fed into the computer program:
1) Two-phase inflow into well; the discharge is then also two phases, so chemical data for both phases must be available.
2) Single-phase inflow into well; the discharge from the well can be either single-phase or two-phase; this model also can also cover springs where the water has not boiled before collection.
3) Springs where the water has boiled and lost steam before the samples were collected.

The WATCH program can also be used to compute the concentrations of the resulting species, activity products and solubility products when the equilibrated fluid is allowed to cool conductively or by adiabatic boiling from the reference temperature to some lower temperature. This is particularly useful in order to evaluate the scaling potential of the fluid. To evaluate the equilibrium minerals in the fluid, several runs of the WATCH program were done for all the wells, G1-G26, using the water sample analyses.

Figure 7 is composed of 4 graphs, representing, respectively, wells number 1, 8, 21, and 24 which were chosen on the base of different location, temperature and structure. The graphs were constructed by the

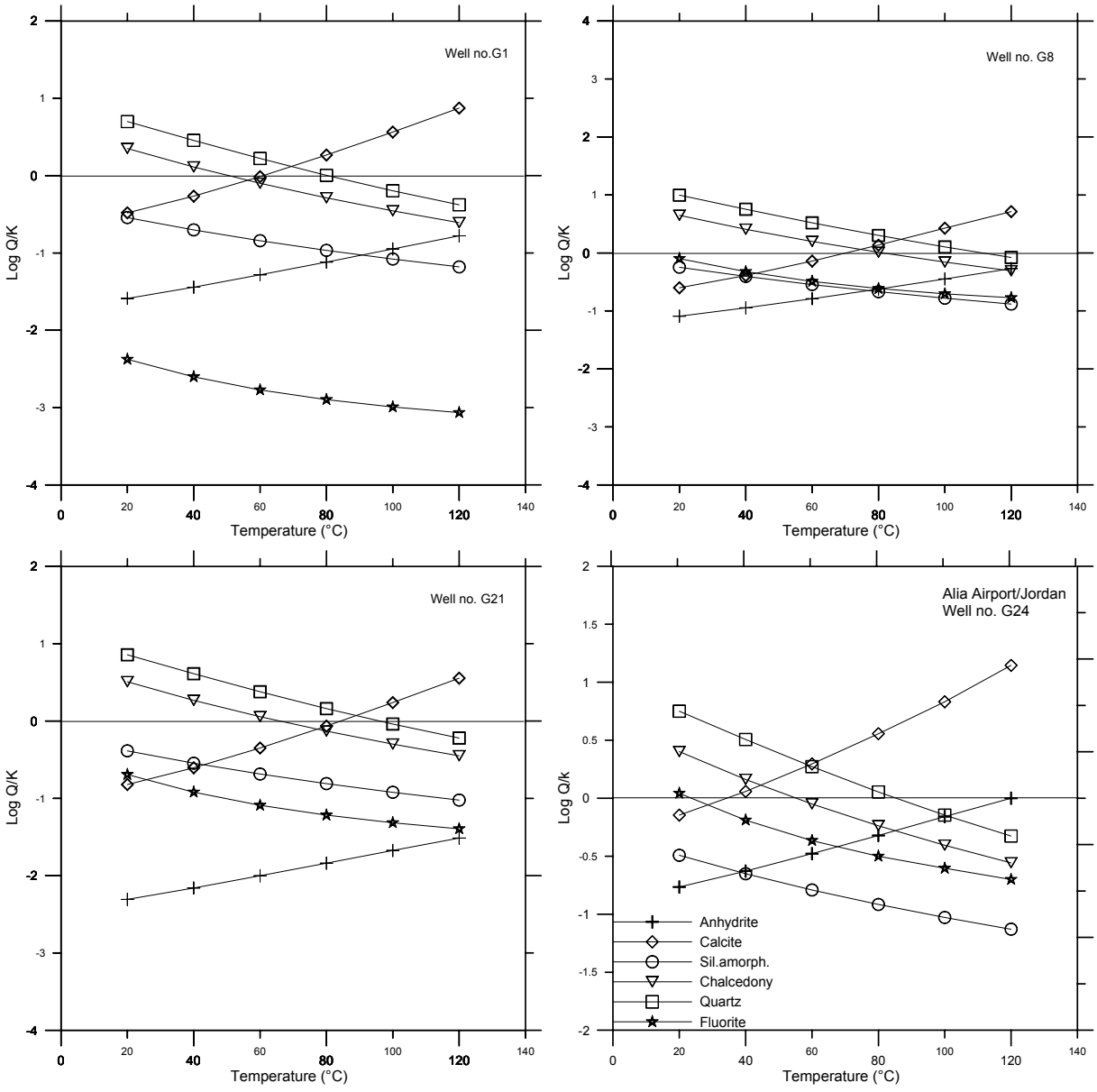

FIGURE 7: Saturation index (log Q/K) vs. temperature calculated with WATCH program for wells G1, G8, G21 and G24 in the Alia area

use of WATCH aqueous speciation program and show logQ/K diagrams for the temperature range 20-120˚C, which are useful to demonstrate reservoir temperatures. The diagrams show the saturation index, log(Q/K), with the mixing equilibrium temperature for each mineral at log(Q/K) = 0. Unfortunately no analysis of Al were available which restricts the number of possible minerals for which it was possible to calculate saturation index.

In the four graphs there is no clear temperature-rock equilibrium reached between all or most of the minerals and the thermal fluids, but in some cases 2-4 of them cross the line at almost the same temperature, indicating near equilibrium. In other cases, the lines cross below the saturation line, which may indicate mixing.

Generally, it can be said that the minerals fluorite and anhydrite are undersaturated. For a few minerals equilibrium is indicated at 60-80˚C and mixing at higher temperatures up to 120˚C, which suggests mixing with cold groundwater. Also, in well 8 there may be re-equalibration of some minerals at a temperature of about 80˚C and mixing at higher temperature is indicated at about 120˚C.

3.5 Mixing evaluations

3.5.1 Evidence of mixing

Water formed by mixing geothermal water and cold groundwater or surface water may possess chemical characteristics which serve to distinguish it from unmixed geothermal water. The reason is that the chemistry of geothermal water is characterized by equilibrium conditions between solutes and alteration minerals, whereas the composition of cold water appears mostly to be determined by the kinetics of the leaching process. The residence time in the bedrock after mixing and the temperature and salinity of the mixed water have an influence on the final chemical composition in the spring discharge. Geothermal waters are often, but not always, much higher in dissolved solids than cold ground and surface waters. Strong conductive cooling of geothermal waters in upflow zones and subsequent reactions with the rock may produce compositional affinities similar to those obtained by leaching subsequent to mixing.

The main chemical characteristics of mixed water, which serve to distinguish them from equilibrated geothermal waters, include relatively high concentrations of silica in relation to the discharge temperature, low pH relative to the water salinity and high total carbonate, at least if the mixing has prevented boiling and the temperature of the hot water component exceeds some 200˚C. Mixed waters tend to be calcite undersaturated and with low calcium/proton activity ratios compared with geothermal waters (Arnórsson, 1985).

The study of the thermal water from Alia strongly suggests mixing of the water to the following reasons:

- There is a disagreement between different geothermometers;
- On the Giggenbach Na-K-Mg triangular diagram, all the samples fall in the partially equilibrated mixed water area;
- On the Giggenbach Cl-SO_4-HCO_3 diagram most of the samples fall in the area for mixed water;
- The mineral equilibria diagrams do not show clear crossing at zero saturation index by any group of minerals at the same temperature;
- There is a nearly linear relationship between chloride and others constituents as suggested by Arnórsson (1985);
- There is a similar trend for the cold and thermal waters plotted in the Schoeller diagram.

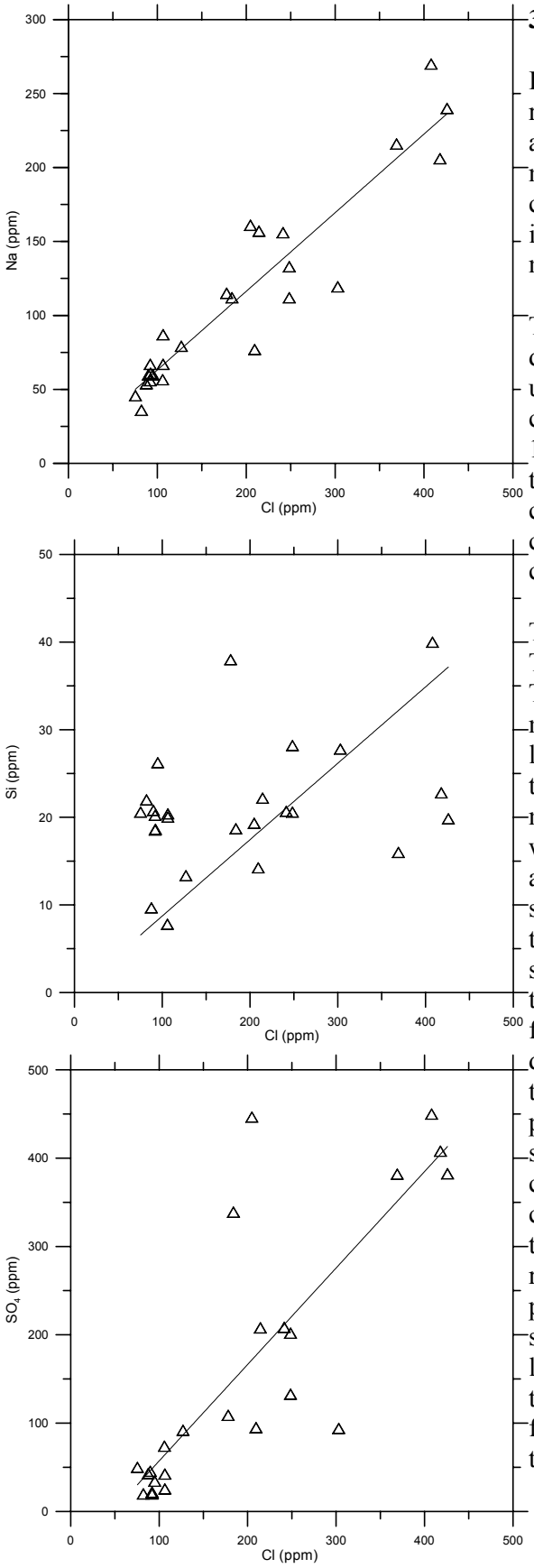

FIGURE 8: The relationships between Cl and some other constituents for the Alia wells

3.5.2 Mixing models

In Figure 8 it can be seen that Na vs. Cl shows a linear relationship, and it can also be said for Si vs. Cl, although it is not as obvious. This is an indication of mixing as suggested by Arnórsson (1985). Sulphate concentrations show a good relationship with chloride in the water except for a few scattered samples, which might be due to waters of different origin.

The **silica-enthalpy mixing model** is a plot of dissolved silica vs. enthalpy of the liquid water and used to estimate the temperature of the hot water component of the mixed water (Truesdell and Fournier, 1977). Enthalpy is used as a coordinate rather than temperature. This is because the combined heat contents of two waters at different temperatures are conserved when those waters are mixed, but the combined temperatures are not.

The Silica-enthalpy mixing model (Fournier and Truesdell, 1977) was applied to the data from Alia. The range of temperature is not very great as the measured temperature in the thermal wells is generally low and not so much higher than the ambient temperature of groundwater in this region. Therefore, many of the samples tend to cluster in one point or within a short range making it difficult to draw a line and estimate reservoir temperature. Therefore the silica-enthalpy mixing model is not very applicable for those waters. Depending on topographical and structural features of the area, the data were split into three groups. Only for data from the central part of the field was there a possibility to draw a line through the data points, but the spread was good enough. In the two other areas the data points tended to cluster in one point. The line failed to intersect the chalcedony saturation curve, but intersects the quartz saturation curve at very high temperatures, about 250˚C, and a connection with the maximum steam loss line gives temperatures of about 165˚C. The results obtained are rather doubtful as they are obtained by selection of a part of the data. Furthermore, the use of the quartz saturation curve may be doubtful for waters at such low temperatures. However, one can conclude that there are some indications in the central part of the field that there may be waters with reservoir temperature exceeding 100˚C.

4. SELFOSS LOW-TEMPERATURE AREA IN ICELAND

The Selfoss geothermal area is a low-temperature field located at the farms Laugardaelir and Thorleifskot in South Iceland (Figure 9), close to the town, Selfoss. The water from the geothermal area has been used for domestic heating of Selfoss since 1948, making the Selfoss district heating service one of the oldest in Iceland. In 1948 when the domestic heating service started, the population was 900 inhabitants, but has since then grown rapidly and is now about 5000.

Exploitation of the area started in 1948, utilizing the free flow of 78˚C hot water from the shallow drillholes near the farm Laugardaelir. When utilization started, the hydrostatic pressure of the geothermal water decreased, causing inflow of cold groundwater. Therefore, new drillholes had to be abandoned soon due to severe cooling. Some electrical resistivity measurements were carried out in the year 1949. Based on the results the Thorleifskot area was favoured over the nearby Laugardaelir area for future production (Bödvarsson, 1949).

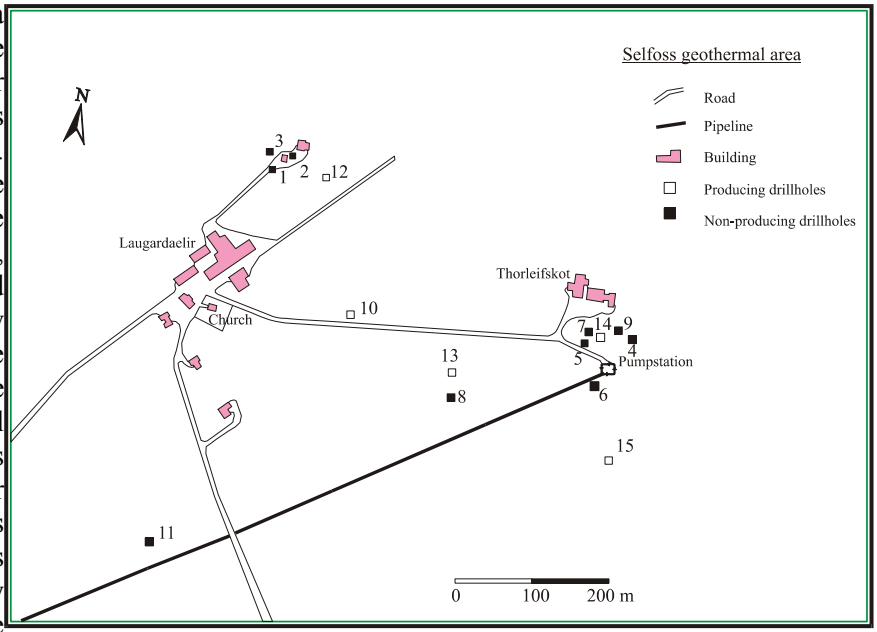

FIGURE 9: The Selfoss geothermal field, S-Iceland

4.1 Geological setting and structural activity

Iceland lies across the crest of a constructive plate boundary, the Mid-Atlantic Ridge, and is composed entirely of volcanic lavas, breccias, tuffs and sediments. The zones of volcanic and tectonic activity are flanked by Quaternary rocks, mainly sequences of subaerial lava flows intercalated by hyaloclastites and morainic horizons at intervals corresponding to glacial conditions (Saemundsson, 1979). The Quaternary formations are bordered by Tertiary subaerial flood basalts. The low-temperature areas in Iceland are located in Quaternary and Tertiary strata.

The geological strata in the Selfoss geothermal area is of Quaternary age, and can be divided (Tómasson and Halldórsson, 1981) into three separate formations. The uppermost formation (0-200 m) consists of the Postglacial lava flow underlain by tillite. The tillite lies unconformably on top of a Quaternary basement, which consists mainly of basaltic lavas with minor sedimentary layers and dolerite intrusives.

4.2 Previous studies and drilling activity

Resistivity measurements in Thorleifskot in the 1970's recognized saline sediments that were partly responsible for the observed low-resistivity field (Georgsson, 1988). Since then there have been made some additional resistivity measurements in order to locate exactly the fractures in the Laugardaelir and Thorleifskot areas (Hersir and Flóvenz, 1982). In 1981, Tómasson and Halldórsson wrote a paper about the cooling of the Selfoss geothermal area. In 1991 one of the UNU Fellows worked on a project dealing with the cooling of the Selfoss geothermal reservoir (Franko, 1991).

Drilling activity started in 1948 near the farm Laugardaelir. After the decline in the hydrostatic pressures due to the inflow of cold groundwater and based on the results from a surface geophysical survey, drilling operations were moved to the farm Thorleifskot, (Figure 9). Between 1950 and 1952 five wells were drilled in this area with depths 150-300 m. From the two first wells THK-1 and 2 the flow was 151 l/s of 82˚C hot water. The cold groundwater was cased off in all of these wells. In 1963 and 1964 wells THK-6, which was 500 m deep and THK-7, which was 490 m deep, were drilled and wells THK-1 and 4 were deepened. A new well, THK-8, was drilled in 1966 down to 450 m depth. In 1972 considerable cooling was observed in the well, and the well was deepened to 738 m. In 1975 and 1976, wells THK-1 to 7 were abandoned and cemented with a pipe for temperature measurements. In 1977 well THK-8 was deepened to a depth of 781 m, and well THK-9 was drilled to a depth of 1334 m. In 1979 well THK-10 was drilled to a depth of 1800 m; but collapsed shortly after drilling at 1100 m depth. In 1980 well THK-11 was drilled to a depth of 2007 m. Well THK-12 was drilled in 1983 at the farm Laugardaelir to a depth of 1936 m. In 1985 well THK-13 was drilled close to well 8 to a depth of 1715 m. In 1989 well THK-14 was drilled at the farm Thorleifskot and is 1430 m deep. Considerable cooling was observed in this well shortly after drilling. To prevent THK-14 from cooling, well THK-9 was cemented with a pipe in 1991. Then in 1996 well THK-15 was drilled and deepened in 1999 from 1280 to 2381 m. It is the last well drilled to date in the Selfoss geothermal area; the presently active production wells in the area are THK-10, THK-12, THK-13, THK-14 and THK-15.

4.3 Characteristics of the thermal fluids

There are two groundwater systems present in the Selfoss geothermal field (Tómasson, 1980), one confined to the Postglacial lava flow and containing a cold groundwater layer (5˚C), and a geothermal system (70-80˚C) mainly confined to the Quaternary basement. The tillite horizon is believed to act as a barrier cap rock between the two systems.

The cooling of the Selfoss low-temperature area was studied by Tómasson and Halldórsson (1981). Pumping of the geothermal water caused lowering of the hydrostatic pressure in the geothermal system, which in turn led to leakage of cold groundwater into the geothermal system. When this vertical leakage reached the subhorizontal aquifer, the water flowed through it to the nearest pumping drillholes. Thus, cooling started in the aquifers and later the reservoir rock was cooled. The thermal water has relatively high chloride content, 108-520 ppm. The chloride is believed to have originated from seawater, dating from early Postglacial time when the area was covered with sea (Tómasson and Halldórsson, 1981). The chloride content varies between drillholes and also with time in the same drillholes, which is believed to be caused by the inflow of cold groundwater with chloride content of 5-10 ppm into the thermal system (Tómasson, 1980).

Table 4 shows the chemical composition for selected wells in the studied area. All the samples were run by the WATCH program and samples from wells 10 and 13 were used for the construction of different diagrams and graphs.

The Schoeller diagram has been used to classify groundwaters and to examine how the samples correlate to each other, and the cold water in the field and Giggenbach´s (1991) triangular diagrams have been used to define both the equilibrium state of the thermal fluids and the type of water with respect to dominant cations and anions.

The **Schoeller diagram** compares the log concentrations of fluid constituents from a number of analyses, with constituents of each analysis connected with a line. The diagram is simply the relationship between the theoretical equilibrium constant and the corresponding activity product in waters at certain temperatures.

TABLE 4: Chemical composition of thermal waters in Selfoss, (concentration in mg/kg)

Sample no.	T (˚C)	pH/˚C	SiO_2	Na	K	Ca	Mg	CO_2 (tot)	SO_4	H_2S	Cl	F	TDS
820119	-	8.6/21	87.6	285	9	71.5	0.02	11.5	152	-	480	0.186	1137
840090	82.5	8.5/21	67.78	156	5.3	22	0.038	28.44	55	.05	221	-	556
850005	108.4	9.0/22	110.3	254	11	32.1	0.013	10.5	126	<.03	354	0.19	924
910008	75	8.6/23	66.6	152	4.6	27	0.08	28	53	<.03	218	0.21	-
910009	75.6	8.7/23	59.9	143	4.1	28	0.07	22	46	<.03	223	0.21	515
930010	70	8.5/24	59.1	132	3.4	25	0.081	28.5	49	<.03	193	0.19	469
930009	74.7	8.6/24	59.8	147	3.7	28	0.064	18.8	51	<.03	229	0.21	546
940004	71.6	8.5/24	64.7	148	3.8	25.7	0.076	30.2	54	<.03	214	0.20	544
940005	71.5	8.6/24	54.8	142	3	28.1	0.073	26.4	46	<.03	216	0.20	519
950049	73.4	8.6/23	66.5	152	4.9	26.1	0.079	29.3	54	.06	227	0.18	537
950048	71.6	8.6/23	55.2	144	3.7	28.7	0.086	22.4	46	<.03	235	0.18	544
960018	72.7	8.6/21	64.4	148	4.2	25	0.086	31.9	55	.12	218	0.22	534
960019	72.2	8.5/22	56.4	143	3.4	29.3	0.091	30.2	49	.08	222	0.22	526
960027	118.8	9.1/21	108.9	276	10.5	35.5	0.007	10.3	142	.27	381	0.21	983
970086	73	8.6/21	66.2	154	4.2	26.2	0.087	34	55	.11	219	0.21	543
970087	70.3	8.6/21	54.1	144	3.1	30.1	0.099	29.8	47	.07	219	0.20	538

Figure 10 shows a Schoeller diagram for four samples chosen from wells 10, 12, 13 and 15, sample numbers, 97-0086, 96-0027, 97-0087 and 97-0088, respectively. The Schoeller diagram suggests mixing between thermal and cold groundwater, and that there exist two types of water. One is higher in sulfate and lower in carbonate, compared to the other.

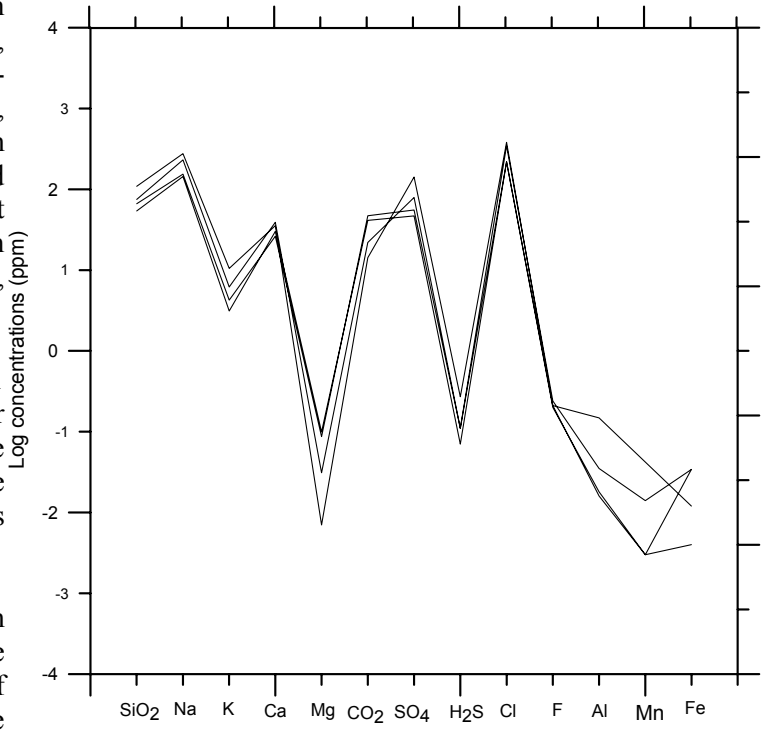

FIGURE 10: Schoeller diagram for thermal waters in Selfoss

Triangular diagrams. Figure 11 shows the $Cl\text{-}SO_4\text{-}HCO_3$ triangular diagram. All the samples plot in the chloride corner of mature waters. The figure also provides initial indications of mixing.

Figure 12 shows Giggenbach's diagram for cations. The data points on the diagram fall into two groups. Most of the samples plot slightly above the equilibrium curve of Arnórsson et al. (1983) and are near equilibrated waters. The diagram yields reservoir temperatures in the range 100-120˚C. Samples no. 960017, 940006 and 850005 from well 12 are outside the equilibrium line, probably due to analytical mistakes. But, anyhow, the water from well 12 is different from the water in all the other wells and is clearly from a different reservoir.

Figure 13 shows that all the samples for Selfoss water are partially equilibrated waters and the reservoir temperatures are indicated between 140-160˚C and t_{km} about 100˚C.

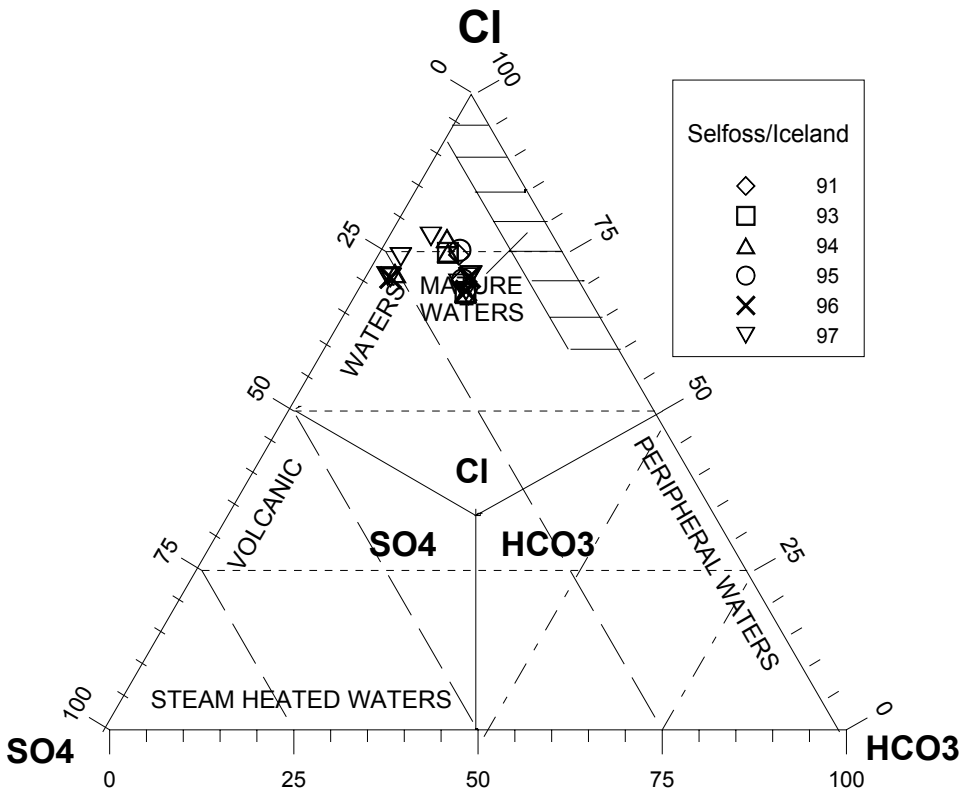

FIGURE 11: Cl-SO_4-HCO_3 diagram for the Selfoss waters

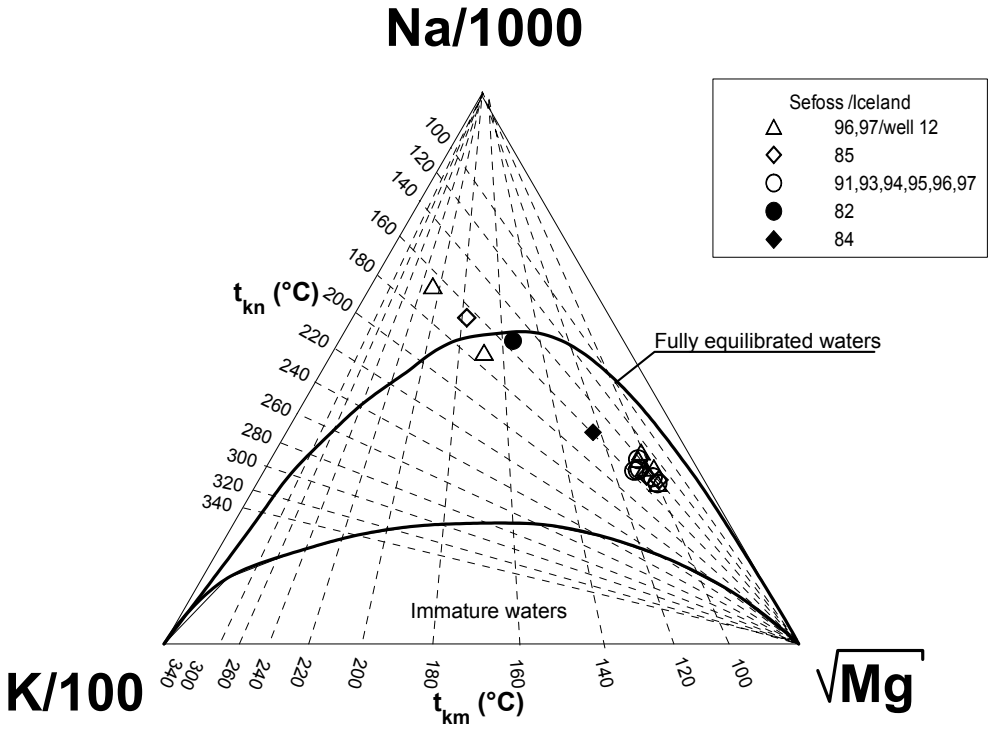

FIGURE 12: The Na-K-Mg diagram for Selfoss, equilibrium curve of Giggenbach (1991)

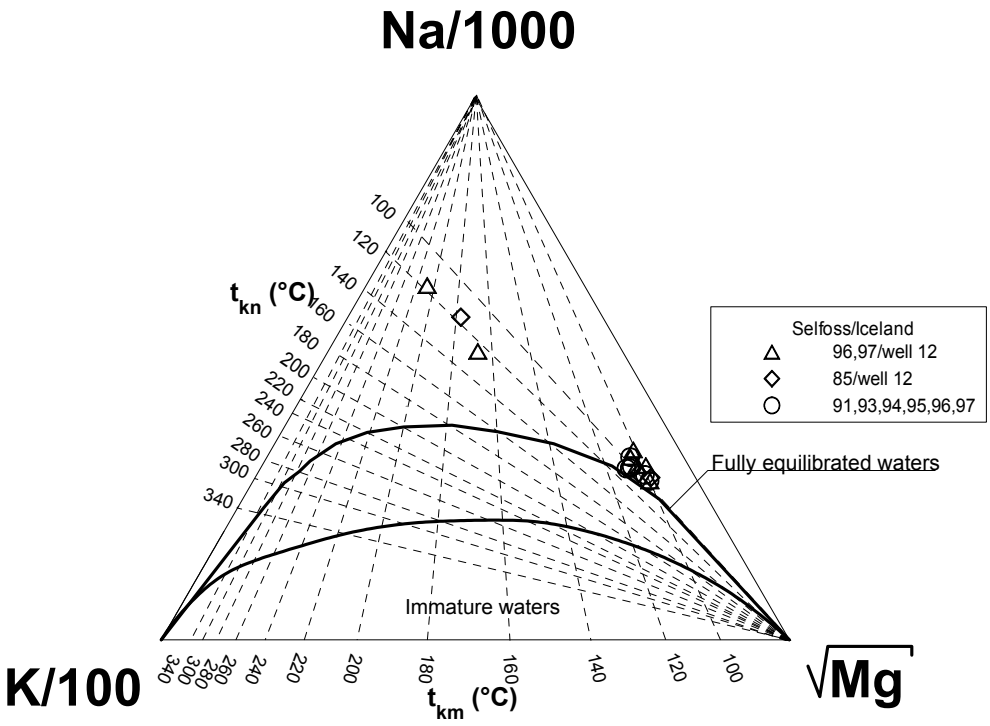

FIGURE 13: The Na-K-Mg diagram for Selfoss, equilibrium curve of Arnórsson et al. (1983)

4.4 Geothermometers

Table 5 shows temperature of different geothermometers calculated from the water analysis from Selfoss. The K-Mg geothermometer is considerably higher than the measured temperature which may be due to the salinity of the mixed water. One would expected it to be considerably lower than the chalcedony and quartz temperatures calculated by Fournier's formula and near to measured temperature.

TABLE 5: Temperature (˚C) based on different geothermometers for the thermal water in Selfoss

Sample no.	$T_{measured}$	$T_{chalcedony}$ 1)	T_{quartz} 2)	T_{Na-K} 3)	T_{Na-K} 4)	T_{K-Mg} 4)
820119	-	102	129	101	154	151
840090	82.5	87	116	106	158	123
910008	75	86	115	98	152	107
910009	77.5	81	110	94	149	106
930010	70	80	109	88	143	99
930009	74.7	81	110	87	142	104
950049	73.4	86	115	102	155	109
950048	71.6	77	106	88	142	100
960018	72.7	85	114	94	148	104
960019	72.2	78	107	83	138	97
970086	73	86	115	92	146	104
970087	70.3	75	105	78	133	94

1) Fournier, 1977
2) Fournier and Potter, 1982
3) Arnórsson et al., 1983
4) Giggenbach, 1988

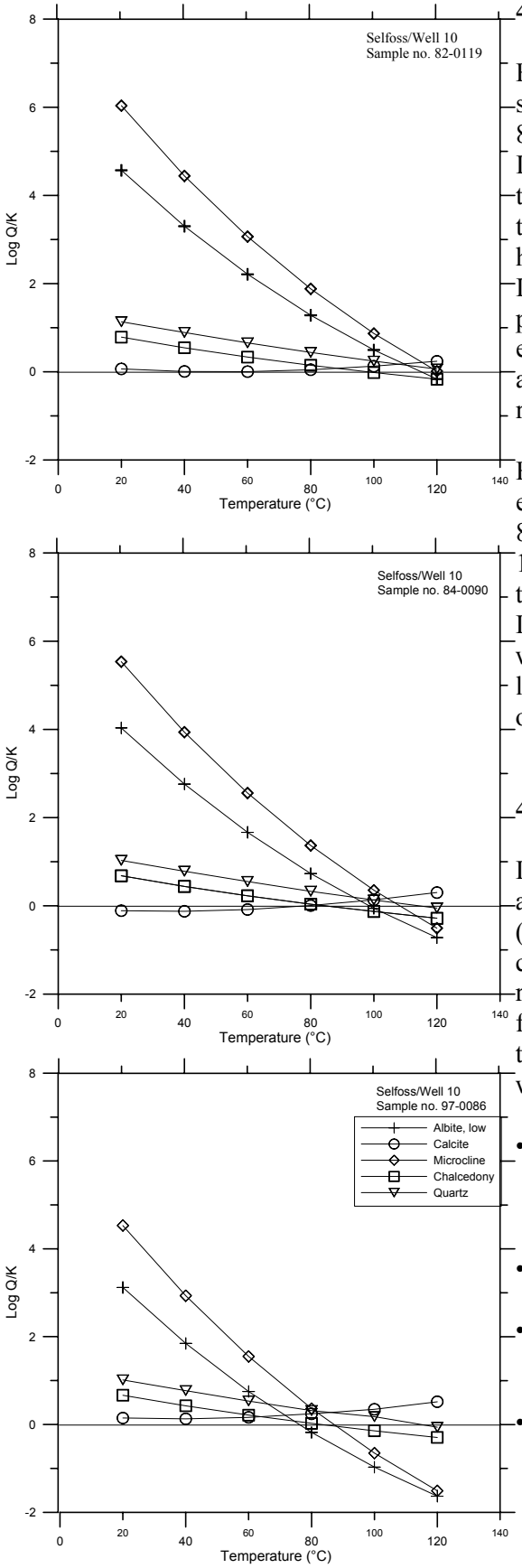

FIGURE 14: Saturation index (log Q/K) vs. temperature calculated with WATCH program for several samples from well 10, Selfoss

4.5 Speciation and equilibrium

Figure 14 is composed of three graphs showing the saturation index, log (Q/K), for samples no. 820119, 840090 and 970086, respectively, from well number 10. If the calculated value for the activity product is equal to the theoretical equilibrium constant for the formation of the corresponding mineral, (log (Q/K) = 0) the mineral has reached equilibrium with the water in the reservoir. If a group of minerals are close to equilibrium at one particular temperature, it means that the water has equilibrated with this group of minerals in the reservoir at the particular temperature, which thus represents the reservoir temperature.

Figure 14 shows that the mineral calcite is in equilibrium for the three samples. For sample no. 840090, many minerals are equilibrated at temperature 100˚C, which yields the reservoir temperature. It's clear that sample 820119 is near equilibrium at about 120˚C. In sample 840090, equilibrium temperatures are lower with some mixing indicated. In sample 970086 much lower reservoir temperatures are indicated with evidence of more mixing.

4.6 Mixing evaluation

In the case of a linear relationship for Cl vs. Na and SO_4, an indication of mixing is suggested by Arnórsson (1985). But there is not so clear relationship between chloride and other components. Figure 15 shows the relation-ship between Cl and other components applied for Selfoss thermal waters. As mentioned earlier here, there is evidence that the ascending hot water has mixed with cold water over time. This evidence is as follows:

- Dilution with time was noticed for some wells and in the shallow feed zones caused by lowering of the hydrostatic pressure in the geothermal system (Tómasson and Halldórsson, 1981);
- Disagreement between different Na/K geothermometers was observed;
- On the Giggenbach Na-K-Mg triangular diagram, some of the samples fell in the mixed water area as shown in Figure 13;
- A near-linear relationship between Cl vs. B, and Cl vs. SO_4 as suggested by Arnórsson (1985), is evidence of mixing in Icelandic geothermal fields. The Selfoss data clearly indicate this linear relationship as shown in Figure 15. Based on this evidence, it seems proper to use mixing models to estimate reservoir temperature in the Selfoss geothermal fields, as well as to gain a better understanding of the processes which may take

place within the geothermal system;

- Log Q/K diagrams in Figure 14 show both lower equilibrium temperatures and increasing signs of mixing over time.

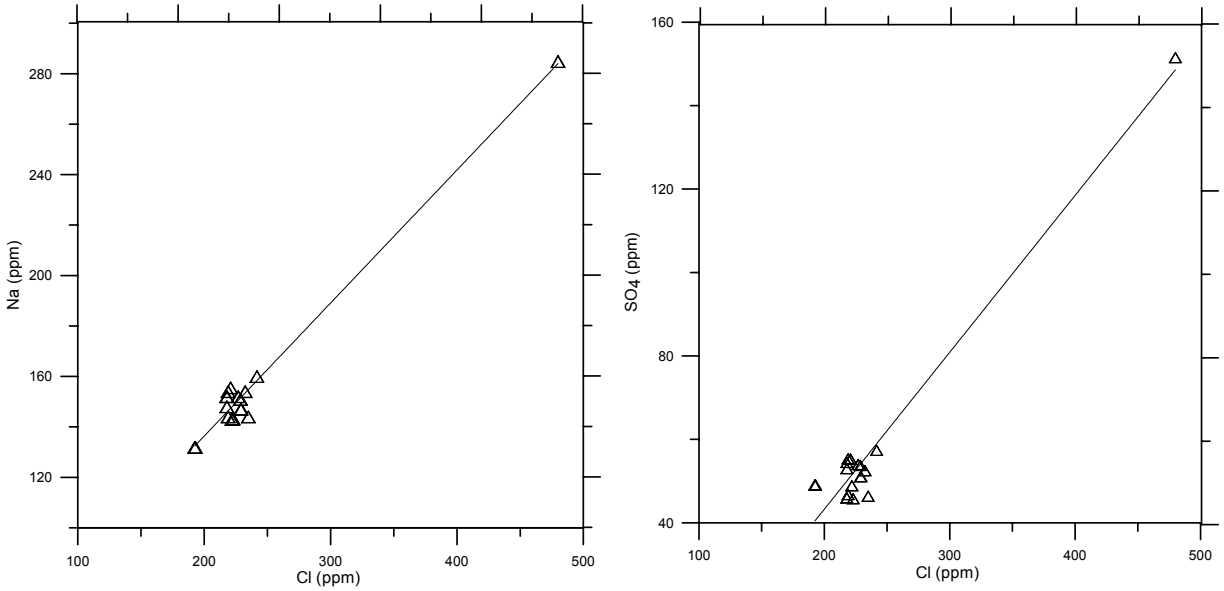

FIGURE 15: Shows the relationship of Cl vs. Na and Cl vs. SO_4 (constituents) for the Selfoss thermal waters

The **Silica-enthalpy mixing model** was applied to the Selfoss data. There are no data available from cold groundwater, only tepid to warm waters. Many of the samples therefore tend to cluster in one point or within a short range making it difficult to draw a line and estimate reservoir temperature. A line connecting the remaining data points failed to intersect the chalcedony saturation curve, probably because the reservoir temperature is too high. Consequently, the data was plotted using the quartz solubility diagram. In that case (Figure 16) the line did intersect the quartz saturation curve at about 150˚C, but could not be connected with the maximum steam loss line. The various geothermometers and log Q/K diagrams indicated that the maximum reservoir temperatures lie within the temperature region 130-160˚C, where either the chalcedony or the quartz saturation curves may be relevant, which may explain that this mixing model fails to give very conclusive results.

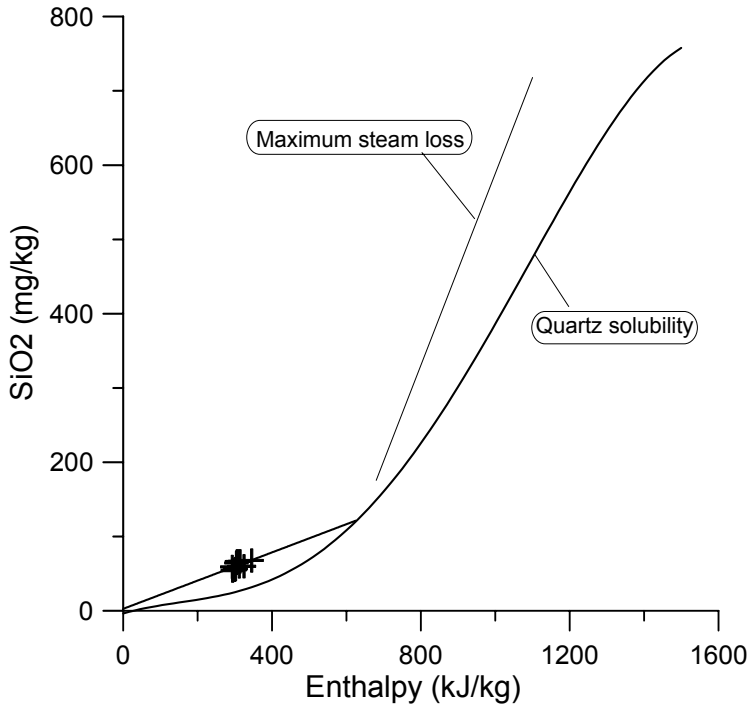

FIGURE 16: Silica-enthalpy mixing model for the thermal waters at Selfoss

5. DISCUSSION AND CONCLUSIONS

The potential and geochemical properties of geothermal waters from the area near Alia airport in Jordan were studied in order to evaluate their possible use for the heating of greenhouses. For comparison geothermal waters from the geothermal field in Selfoss, Iceland, with a long and well known production history, were studied with similar geochemical methods. Speciation in the waters was calculated by the computer program WATCH and many different graphical presentation applied giving information about mineral equilibrium and estimates of the possible reservoir temperature by the use of different geothermometers. Evaluation of mixing was made in both study areas by different geochemical methods. Chemical analyses from several wells in Selfoss over several years were selected for interpretation, mainly from wells 10 and 13. Several wells in Jordan were also chosen, mainly wells G1, 6, 8, 13, 14, 18, 21 and 24, based on high temperatures and mineral equilibrium. The chemical composition of geothermal water in Selfoss is different from that in Jordan; no definite equilibrium temperature can be appointed. The latter is rich in carbonate and the pH is less than 7. It seems to act as meteoric water. According to the mineral saturation index, none of the minerals are in equilibrium in Jordan; no definite mineral equilibrium temperature can be pinpointed. For the Selfoss thermal water, increased inflow of cold water is displayed by time. The mineral calcite is in equilibrium for the three samples 820119, 840090 and 970086, respectively, for well 10. Sample 820119 is near equilibrium at about 120˚C, whereas in sample 840090, equilibrium temperatures are lower due to some mixing. In sample 970086, much lower reservoir temperatures are indicated with evidence of more mixing. The maximum reservoir temperature predicted by calculation of various geothermometers is more than 100˚C in Jordan, while for Selfoss geothermal field it is in the range 130-160˚C.

For the Jordan waters, there were no available analyses of aluminum which restricted considerably the number of minerals for which it was possible to calculate equilibrium conditions. All the samples show evidence of considerable mixing, but there are indications for the existence of geothermal water up to about 100˚C.

Concerning the question of the possible use of geothermal energy in Jordan to heat greenhouses, there appears to be a potential for such use. More research is needed to assess the energy potential, but the temperature of the waters appears to be sufficiently high. Due to the bicarbonate type of water, care has to be taken in the design of the system in order to prevent problems due to corrosion and scaling. An extensive regional survey is needed as well as more detailed studies including temperature logging of the wells, deep water sampling, measurement of more components in water samples as aluminium, heavy metals and stable isotopes.

ACKNOWLEDGMENTS

I would like to express my gratitude to Dr. Ingvar Fridleifsson, director, for providing me the opportunity to attend the UNU Geothermal Training Programme. I am very grateful to my advisor, Mrs. Hrefna Kristmannsdóttir for her assistance, guidance and discussions during preparation of the report. Thanks are due to Dr. Stefán Arnórsson for two weeks of training in thermodynamics and his excellent lectures. My gratitude goes to Mrs. Steinunn Hauksdóttir for her help and willingness to assist me.

Thanks go to Mr. Lúdvík S. Georgsson for all the care and generous help and advice during the whole training period. And, thanks to Mrs. Gudrún Bjarnadóttir for her wonderful care.

I wish to give my thanks to all lecturers and staff members at Orkustofnun for their comprehensive presentations and willingness to share their knowledge and experience. And I extend my thanks to the people of Iceland for their generous hospitality.

I am also indebted to Mr. Hiari ma´n, the general director, Mr. Darwish Jaser, the director of the geology directorate, and to Mr. Mohammed Okour, the head of the geochemistry division from the Natural Resources Authority in Jordan, who supported and encouraged me to attend the course. Also to Mr. Ali Swarieh for his help.

My deep appreciation is due to my mum and my wife Ghada for their love and inspiration.

REFERENCES

Abu Ajamieh, M., 1973: *Gravity map of portions of Jordan, scale 1:250,000.* Natural Resources Authority, Amman, Jordan.

Arnórsson, S., 1975: Application of the silica geothermometer in low-temperature hydrothermal areas in Iceland. *Am. J. of Sci.,* 275, 763-783.

Arnórsson, S., 1985: The use of mixing models and chemical geothermometers for estimating underground temperature in geothermal systems. *J. Volc. Geotherm. Res., 23,* 299-335.

Arnórsson, S., 1991: Geochemistry and geothermal resources in Iceland, In: D´Amore, F. (co-ordinator), *Applications of geochemistry in geothermal reservoir development.* UNITAR/UNDP publication, Rome, 145-196.

Arnórsson, S., Gunnlaugsson, E., and Svavarsson, H., 1983: The chemistry of geothermal waters in Iceland III. Chemical geothermometry in geothermal investigations. *Geochim. Cosmochim. Acta*, *47*, 567-577.

Bender, F., 1974: *Geology of Jordan.* Bortraeger, Berlin, 196 pp.

Bjarnason, J.Ö., 1994: *The speciation program WATCH, version 2.1.* Orkustofnun, Reykjavík, 7 pp.

Bödvarsson, G., 1949: *Resistivity measurements, Laugardaelir, Flói*. Orkustofnun, report (in Icelandic), 14 pp.

Demange J., Gauthier, B., Martin, G., and Tournaye, D., 1992: *Study for the use of geothermal resources for greenhouse heating, South Amman Zone, Kingdom of Jordan.* Comp. Franc. De Geothermice, 141 pp.

Fournier, R.O., 1977: Chemical geothermometers and mixing model for geothermal systems. *Geothermics, 5,* 41-50.

Fournier, R.O., and Potter, R.W. II, 1982: A revised and expanded silica (quartz) geothermometer. *Geoth. Res. Council Bull., 11-10*, 3-12.

Fournier, R.O., and Truesdell, A.H., 1973: An empirical Na-K-Ca geothermometer for natural waters. *Geochim. Cosmochim. Acta*, *37*, 1255-1275.

Franko, J. 1991: *The cooling of the Selfoss geothermal reservoir in southern Iceland.* UNU G.T.P., Iceland, report 6, 31 pp.

Futyan, A., 1968: *Stratigraphy of Belqa 2 (B2) and Belqa 3 (B3) of formations in Jordan and the origin of their bitumen.* Natural Resources Authority, Amman, unpublished report.

Georgsson, L. S., 1988: *Geothermal activity and resistivity around Selfoss*. Orkustofnun, Reykjavík, notes from a summary meeting of Hitaveita Selfoss July 1988, report (in Icelandic), 6 pp.

Giggenbach, W. F., 1981: Geothermal mineral equilibria. *Geochim. Cosmochim. Acta*, *45*, 393-410.

Giggenbach, W.F., 1988: Geothermal solute equilibria. Derivation of Na-K-Mg-Ca geoindicators. *Geochim. Cosmochim. Acta, 52,* 2749-2765.

Giggenbach, W. F., 1991: Chemical techniques in geothermal exploration. In: D'Amore, F. (coordinator), *Application of geochemistry in geothermal reservoir development*. UNITAR/UNDP publication, Rome, 119-142.

Hersir, G., and Flóvenz, Ó.G., 1982: *Resistivity measurements at Selfoss*. Orkustofnun, Reykjavík, report OS-8267/JHD-13B (in Icelandic), 29 pp.

Jaser, D., 1986: *The geology of Khan ez Zabib, map sheet no.3253.* Natural Resources Authority,geology directorate, Amman, Jordan.

Nicholson, K., 1988: *Geochemistry of geothermal fluids: An introduction.* Geothermal Institute, University of Auckland, New Zealand, report, 87 pp.

Saemundsson, K., 1979: Outline of the geology of Iceland. *Jökull 29*, 7-28.

Swarieh, A., 1992: *Thermal boreholes near Alia airport.* Natural Resources Authority, geology directorate, Jordan, unpublished report.

Tómasson, J., 1980: Selfoss geothermal area, S-Iceland. The using of chlorine as an indicator of an inflow of cold groundwater into the geothermal reservoir. *Proceedings of 3rd International Symposium on Water-Rock Interaction, Edmonton, Canada, July 1980,* 107-109

Tómasson, J., and Halldórsson, G., 1981: The cooling of the Selfoss geothermal area, S-Iceland. *Geothermal Resources Council, Transactions 5,* 209-212.

Truesdell, A.H., 1991: Effects of physical processes on geothermal fluids. In: D'Amore, F. (coordinator), *Application of geochemistry in geothermal reservoir development.* UNITAR/UNDP publication, Rome, 71-92.

Truesdell, A.H., and Fournier, R.O., 1977: Procedure for estimating the temperature of a hot water component in a mixed water using a plot of dissolved silica vs. enthalpy. *U.S. Geol. Survey J. Res., 5,* 49-52.